

CHARM: Collaborative Harmonization across Arbitrary Modalities for Modality-agnostic Semantic Segmentation

Lekang Wen¹, Jing Xiao^{2*}, Liang Liao³, Jiajun Chen¹, Mi Wang¹,

¹State Key Laboratory of Information Engineering in Surveying, Mapping and Remote Sensing, Wuhan University

²School of Artificial Intelligence

³Hangzhou Institute of Technology, Xidian University

wenlk3@whu.edu.com, jing@whu.edu.com, liaoliang1@xidian.edu.cn, jiajunchen@whu.edu.com, wangmi@whu.edu.com,

Abstract

Modality-agnostic Semantic Segmentation (MaSS) aims to achieve robust scene understanding across arbitrary combinations of input modality. Existing methods typically rely on explicit feature alignment to achieve modal homogenization, which dilutes the distinctive strengths of each modality and destroys their inherent complementarity. To achieve cooperative harmonization rather than homogenization, we propose CHARM, a novel complementary learning framework designed to implicitly align content while preserving modality-specific advantages through two components: (1) Mutual Perception Unit (MPU), enabling implicit alignment through window-based cross-modal interaction, where modalities serve as both queries and contexts for each other to discover modality-interactive correspondences; (2) A dual-path optimization strategy that decouples training into Collaborative Learning Strategy (CoL) for complementary fusion learning and Individual Enhancement Strategy (InE) for protected modality-specific optimization. Experiments across multiple datasets and backbones indicate that CHARM consistently outperform the baselines, with significant increment on the fragile modalities. This work shifts the focus from model homogenization to harmonization, enabling cross-modal complementarity for true harmony in diversity.

1 Introduction

Multimodal Semantic Segmentation (MSS) aims to leverage complementary features from multiple visual modalities to achieve robust scene understanding, particularly under adverse conditions, *e.g.*, heavy fog, nighttime, and rain. For instance, in autonomous driving scenarios under rainy conditions, RGB-based perception often suffers from substantial degradation due to reduced visibility. In contrast, auxiliary modalities such as LiDAR and Depth sensors can provide geometry-aware cues that compensate for the perception limitations of RGB, thereby improving driving safety. Most existing MSS methods follow an $X+A$ paradigm, where X denotes as a designated primary modality and A represents one (Tan et al. 2024; Dong et al. 2024; Wei et al. 2025; Zhang et al. 2025a; Yang et al. 2025) or multiple auxiliary modalities (Zhang et al. 2023a; Brödermann et al. 2023; Li et al. 2024; Wan et al. 2024; Zhang et al. 2025b). However, this paradigm inherently prioritizes the primary modality,

which suppresses the contribution of auxiliary modalities, leading to significant performance degradation when the primary modality is unavailable or compromised.

Modality-agnostic Semantic Segmentation (MaSS) has emerged to enable robust performance under diverse and incomplete modality configurations. Early efforts tackled multimodal imbalance by employing modality dropout (Zhang et al. 2022, 2023b; Shi et al. 2024; Maheshwari, Liu, and Kira 2024), which randomly omits input sources during training. However, it may be insufficient to ensure effective representation learning for non-dominant or fragile modalities. Recent methods (Chen, Zhao, and Bruzzone 2024; Zheng, Lyu, and Wang 2025; Zheng et al. 2024a,b, 2025) have shifted toward feature alignment, enforcing cross-modal feature consistency through explicit constraints, *e.g.*, KL divergence. MAGIC (Zheng et al. 2024a) groups modalities into robust and fragile sets and aligns their features with a cosine-based loss. Any2Seg (Zheng, Lyu, and Wang 2025) incorporates semantic guidance from vision-language models to enhance alignment, while AnySeg (Zheng et al. 2025) distills all modality features toward informative representation, improving performance in fragile-modal combinations. Although these alignment-based methods have shown to better handle combinations involving robust modalities, their reliance on explicit alignment often suppress modality-specific characteristics, leading to homogenized representations and reduced cross-modal complementarity.

As illustrated in Fig. 1(a), different modalities could capture distinct aspects of the same scene, resulting in inherent misalignment. For example, the building missed in LiDAR while the Lane marking is only available in RGB. Explicit alignment-based methods as shown in (b) homogenizes these multimodal features by enforcing convergence across inherently divergent distributions. This process weakens modality-specific strengths, as RGB’s rich information is diluted to match achromatic patterns of LiDAR for the building case, and LiDAR’s precise spatial cues are suppressed in the car case as shown in (d). This limitation motivates us to pursue a novel approach that preserves the distinct characteristics of each modality while enabling effective collaboration, namely to harmonize modalities under two principles: 1) modalities should coordinate through mutual understanding of each other, enabling the system to jointly model comprehensive scene information across

*Corresponding author

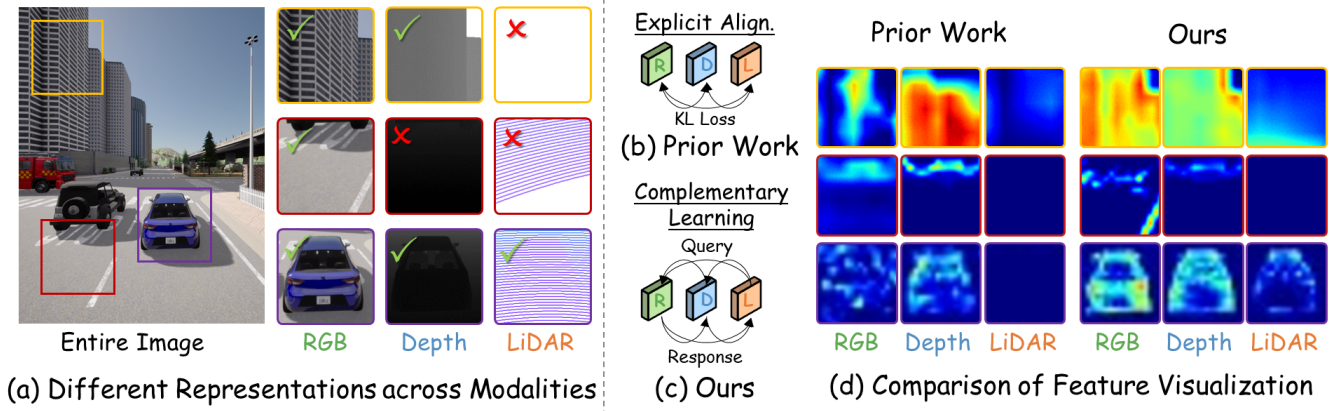


Figure 1: Example of modality misalignment and comparison of designed methods for MaSS. (a) Examples of content variations in different modalities; (b) Prior works use explicit alignment (*e.g.*, KL divergence) that forces feature homogenization; (c) Our approach employs complementary learning through query and response to discover modality-interactive correspondences; (d) features of RGB and LiDAR are suppressed in prior work while in our work the features show their boosted specific information.

modalities; 2) the complementary features of each modality should be actively stimulated and reinforced during the multi-modal interaction, rather than suppressed by uniform alignment constraints.

In this work, we propose **Collaborative Harmonization across ARbitrary Modalities (CHARM)**, a MaSS framework that enables synergistic feature interaction while preserving modality-specific strengths. The core of CHARM lies in two aspects according to the above principles. Firstly, a fundamental unit, named **modality Mutual Perception Unit (MPU)**, is proposed to explore the complementarity among modalities through cross-modal attention, where each modality simultaneously serve as queries and contexts to the others, enabling the discovery of modality-interactive correspondences at each feature scale. Second, two pathways are designed to systematically balance collaborative learning of all modalities (principle 1) with individual enhancement (principle 2): **Collaboration Learning strategy (CoL)** for joint optimization that dynamically adapts cooperation based on each modality’s robustness, and **Individual Enhancement strategy (InE)** that provides protected learning spaces with the robustness guidance for individual modalities to stimulate their full potential.

The main contributions of this work are threefold:

- We identify the fundamental limitation of modality homogenization in existing explicit alignment strategy for MaSS on suppressing the modal-specific features, and propose a cooperative paradigm that enables effective complementarity across modalities;
- We designed a complementary learning framework, *i.e.*, CHARM, with a fundamental unit MPU to explore the complementarity across modalities, and two strategies of CoL for collaborative learning of all modalities and InE for individual enhancement by mutually learning from other modality;
- Extensive experiments demonstrate that CHARM significantly improves the effectiveness of each modality and

their various combinations, ensuring robust MaSS performance that consistently surpasses advanced baselines.

2 Related Work

2.1 Multimodal Semantic Segmentation

MSS aims to enhance segmentation accuracy and robustness by integrating information from different sensors. Previous approaches focused on fusing RGB with auxiliary modalities, such as Depth (Feng et al. 2024; Wei et al. 2025), Event (Alonso and Murillo 2019; Xia et al. 2023), LiDAR (Tan et al. 2024; Zhang et al. 2025a), thermal (Dong et al. 2024; Yang et al. 2025), and polarization (Mei et al. 2022). With the advancement of sensor technologies, dual-modal semantic segmentation has expanded to multimodal semantic segmentation, where approaches can be categorized into symmetric branch distribution (Liang et al. 2022; Reza, Prater-Bennette, and Asif 2024; Li et al. 2024) and asymmetric branch distribution (Brödermann et al. 2023; Wan et al. 2024; Zhang et al. 2025b) architectures. The former treats all modalities equally, such as MMSFormer (Reza, Prater-Bennette, and Asif 2024), which achieves semantic segmentation by concatenating all multimodal features and fusing them through linear layers. The latter designates the most robust modality as the primary modality while treating others as auxiliary inputs. For instance, GFBN (Gao et al. 2024) uses RGB as the primary modality and incorporates other modalities to achieve arbitrary-modal semantic segmentation.

MSS methods demonstrate exceptional performance when all input modalities are in the normal state. However, they are generally designed for a specific modality combination, limiting their performance when applied to MaSS with any modalities missing or degraded.

2.2 Modality-agnostic Semantic Segmentation

MaSS aims to achieve robust performance across diverse and incomplete modality configurations. Initial approaches addressed multimodal imbalance through modality dropout

strategies (Sharma and Hamarneh 2020; Zhang et al. 2022, 2023b; Shi et al. 2024; Maheshwari, Liu, and Kira 2024), which randomly exclude input modalities during training. Nevertheless, such strategies may prove inadequate for ensuring effective representation learning of non-dominant or vulnerable modalities. Contemporary methods (Wang et al. 2023; Liu et al. 2024; Chen, Zhao, and Bruzzone 2024; Zheng, Lyu, and Wang 2025; Zheng et al. 2024a,b, 2025) have pivoted toward feature alignment paradigms, imposing cross-modal feature consistency via explicit constraints such as KL divergence. Notably, MAGIC (Zheng et al. 2024a) categorizes modalities into robust and fragile subsets, aligning their features using cosine-based loss functions. Any2Seg (Zheng, Lyu, and Wang 2025) leverages semantic guidance from vision-language models to enhance cross-modal alignment, whereas AnySeg (Zheng et al. 2025) employs knowledge distillation to guide all modality features toward more informative representations, thereby improving performance in fragile-modal combinations.

While current alignment-centric approaches demonstrate superior handling of combinations involving robust modalities, their dependence on explicit alignment tends to suppress modality-specific characteristics. This leads to homogenized representations that diminish cross-modal complementarity, potentially limiting the full exploitation of multimodal information.

3 Methodology

3.1 Problem Formulation of MaSS

Following the common setting, we consider a modality set \mathcal{M} comprising M modalities. Let $\mathcal{I} = \{I_m\}_{m \in \mathcal{M}}$ represent the full multimodal input, and S denote the corresponding segmentation labels. During training, all modalities are assumed to be accessible, while during inference, only a subset $\mathcal{I}^{\text{sub}} \subseteq \mathcal{I}$ is available due to sensor failures, environmental variability, or cost constraints. The goal of MaSS is to learn a segmentation model that maintains robust and accurate under arbitrary modality combinations, particularly in the presence of missing modalities.

Typically, models trained with full multimodal supervision suffers significant performance degradation when certain modalities are missing. To mitigate this issue, existing approaches employ a twofold solution: (1) random modality dropout during training to simulate diverse incomplete modality scenarios, generating input subsets \mathcal{I}_{sub} , and (2) cross-modal feature alignment to ensure representation consistency across modalities. The model Φ is then optimized to handle various modal combinations by minimizing:

$$\min_{\Phi} \mathcal{L}_{\text{MaSS}} = \lambda_{\text{seg}} \mathcal{L}_{\text{seg}}(\Phi(\mathcal{I}_{\text{sub}}), S) + \lambda_{\text{align}} \sum_{(m, m') \in \mathcal{P}} \mathcal{L}_{\text{align}}(f_m, f_{m'}), \quad (1)$$

where $\mathcal{P} = \{(m, m') | m, m' \in \mathcal{M}, m \neq m'\}$ represents all distinct modality pairs, f_m and $f_{m'}$ denote the features from modalities m and m' , \mathcal{L}_{seg} is the cross-entropy loss for segmentation, $\mathcal{L}_{\text{align}}$ is the similarity loss for multimodal feature alignment, and $\lambda_{\text{seg}}, \lambda_{\text{align}}$ are balancing coefficients.

3.2 Framework Overview

The framework of the proposed CHARM is shown in Fig. 2, where we formulate MaSS as a cooperative harmonization problem and solve it with a two-pathway synergistic process. MPU is the core module that can accept arbitrary numbers and types of multimodal features as queries and contexts, enabling each querying modality to perceive the content of others during learning. It facilitates the discovery of modality-interactive correspondences, resulting in implicit alignment without explicit constraints. These aligned modalities can, in turn, complement and enhance each other.

To leverage MPU effectively, CHARM integrates two cooperative pathways: CoL uses extracted multimodal features as queries and contexts to mine modality-interactive correspondences between multiple modalities, enabling model to learn complementary information and maximize synergy across modalities; InE employs individual modal features as queries and contexts to mine interactive responses within single modalities. Although CoL effectively enhances complementary capabilities, the issue of modal imbalance potentially suppress the fragile modalities. In contrast, InE provides a protective learning space for all modalities, thereby improving the individual potential of each modality.

Taking four modalities of RGB (R), Depth (D), Event (E), and LiDAR (L) modalities as an example, CHARM packs all input images I_m into a mini-batch for efficient parallel computation. A shared-weight encoder F extract features for each modality independently across each scale:

$$\{f_m^i\}_{i=1}^4 = F(I_m). \quad (2)$$

It is important to note that CoL and InE operate in couples: the feature f_m^i from each modality is processed through both pathways to generate a modal-collaborative feature f_{CoL}^i and a modal-enhanced feature f_{InE}^i . These features are then fed into a segmentation head to produce the modal-collaborative prediction \hat{S}_{CoL} and the modal-enhanced prediction \hat{S}_{InE} for joint optimization, respectively.

3.3 Mutual Perception Unit

To discover modality-interactive correspondences, MPU enables mutual perception across modalities through iterative query, where each modality's features serve as both queries (Q) and contexts (K, V) for the others. Designed to be modality-agnostic, MPU can robustly handle arbitrary modality combinations during inference. For multi-modal imagery, it introduce a windowed attention design to balance a large cross-modal receptive field with computational efficiency.

To further enhance cross-modal interaction, multiple MPU blocks are employed in CHARM, where each block follows a specific structure shown in Fig. 3. Specifically, $f_{m \rightarrow se}^i$ is partitioned into J windowed modal semantic features $\{x_m^{i,j}\}_{j=1}^J$, while $f_{se \rightarrow l}^i$ is partitioned into J windowed semantic features $\{x_{se}^{i,j}\}_{j=1}^J$. Each $\{x_m^{i,j}\}_{j=1}^J$ has modality-specific weight matrices for generating Key and Value, thus

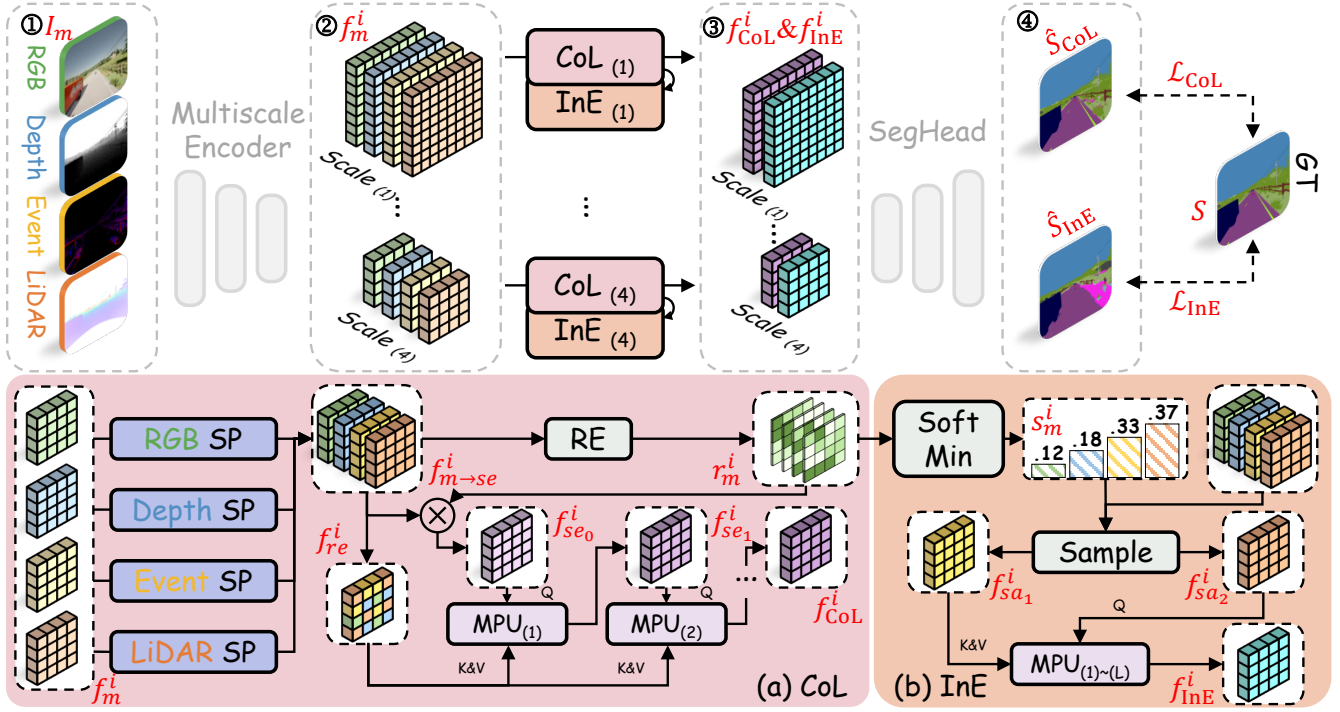


Figure 2: The overall framework of CHARM. At each scale, the encoder extracts multimodal features. CoL and InE are coupled when training and added between scales to fuse them progressively and input into the SegHead for segmentation.

the generation process of Q, K, V is formulated as:

$$\begin{aligned} Q_{i,j} &= x_{se}^{i,j} W^Q, \\ K_{i,j} &= \{x_m^{i,j} W_m^K\}_{m \in \mathcal{M}}, \\ V_{i,j} &= \{x_m^{i,j} W_m^V\}_{m \in \mathcal{M}}. \end{aligned} \quad (3)$$

These serve as inputs for the Window Multi-Head Attention (W-MHA) (Liu et al. 2021), outputting interacted windowed semantic features $\{x_{se}^{i,j}\}$, which are finally assembled through reverse partition to obtain the semantic feature $f_{se_l}^i$. Shifted window partitioning is introduced to enable cross-window connections by shifting during adjacent MPU blocks. Different from addition or concatenation fusion, MPU naturally accommodates arbitrary numbers of modalities as input, and the separable Q, K, V relationships prevent any single modality from dominating the learning process, ensuring balanced multimodal interaction. In the both pathways described in the following, L MPU blocks are embedded within both pathways at each scale. In CoL, MPU optimally integrates simultaneous multi-modal inputs, while in InE, it enables each modality to learn modality-interactive correspondences.

3.4 Collaboration Learning Strategy

As shown in Fig. 2(a), in CoL, the modal features $\{f_m^i\}_{m \in \mathcal{M}}$ at each scale are first projected to a semantic space via Semantic Projectors (SP), yielding $\{f_{m \rightarrow se}^i\}_{m \in \mathcal{M}}$. Each SP is a modality-specific sequential block consisting of three depth-wise convolutions with kernel sizes of 11×11 , 7×7 , and 3×3 , followed by a 1×1 point-wise convolution, as described in Fig. 4. To quantify

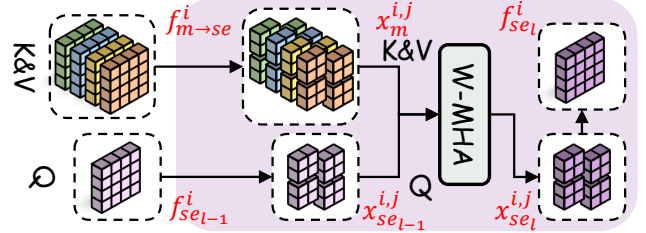


Figure 3: Structure of Mutual Perception Unit (MPU).

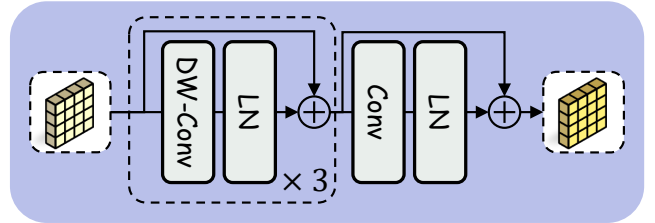


Figure 4: Structure of Semantic Projector (SP).

the reliability of each modality at every pixel, a Robustness Evaluator (RE), implemented as a 1×1 point-wise convolution, is used to compute the pixel-wise robustness scores $\{r_m^i\}_{m \in \mathcal{M}}$. These scores are then used to compute the initial semantic feature $f_{se_0}^i$ via a robustness-weighted summation across modalities:

$$f_{se_0}^i = \sum_{m \in \mathcal{M}} r_m^i f_{m \rightarrow se}^i, \quad (4)$$

which serves as the Query for the first MPU block. To reduce computational cost and modal dependency, modality-reassembled feature f_{re}^i is randomly selected from the corresponding position across all modality-specific semantic features, serving as the Key and Value for MPU block to enable fine-grained, cross-modal interaction. Through iterative processing across MPU blocks, the semantic features are progressively refined, ultimately generating the fused modal feature f_{CoL}^i . This design encourages complementary information exchange by enforcing cross-modal interactions, allowing modalities to compensate for each other's deficiencies in a content-aware and position-sensitive manner.

3.5 Individual Enhancement Strategy

As shown in Fig. 2(b), in InE, the modality robustness scores $\{r_m^i\}_{m \in \mathcal{M}}$ are averaged to obtain scalar values $\{\bar{r}_m^i\}_{m \in \mathcal{M}}$, which are then normalized through *SoftMin* to derive sampling probabilities $\{s_m^i\}_{m \in \mathcal{M}}$:

$$s_m^i = \text{SoftMin}(\bar{r}_m^i), m \in \mathcal{M}. \quad (5)$$

Subsequently, fragile modality-biased sampling is employed based on $\{s_m^i\}_{m \in \mathcal{M}}$ to extract complete modal semantic features $f_{sa_1}^i$ and $f_{sa_2}^i$ that serve as Q, K, V for MPU blocks, generating the enhanced modal feature f_{InE}^i . This fragile modality-biased learning strategy emphasizes the potential of fragile modalities by providing them with more learning opportunities. Since the input modal features are complete and do not incorporate information from other modalities, InE implements protective learning for individual modalities. The combination of individual modal features and mutual perception facilitates modalities to discover complementary information from each other and promotes implicit alignment across modalities.

3.6 Model Training and Inference

As output features from CoL and InE have the same shape, they are packaged as input to SegHead for parallel segmentation. The loss functions \mathcal{L}_{CoL} and \mathcal{L}_{InE} both use cross-entropy loss for supervised training:

$$\begin{aligned} \mathcal{L}_{CoL} &= - \sum_{p \in S} S(p) \log(\hat{S}_{CoL}(p)), \\ \mathcal{L}_{InE} &= - \sum_{p \in S} S(p) \log(\hat{S}_{InE}(p)), \end{aligned} \quad (6)$$

where p is the pixel index for segmentation map S . The MaSS optimization is then simplified as:

$$\min_{\Phi} \mathcal{L}_{MaSS} = \lambda_{CoL} \mathcal{L}_{CoL} + \lambda_{InE} \mathcal{L}_{InE}, \quad (7)$$

where \mathcal{L}_{CoL} and \mathcal{L}_{InE} denote the collaborative learning loss and modal enhancement loss, respectively. λ_{CoL} and λ_{InE} are balancing coefficients.

In inference phase, the model follows a process similar to CoL, with the difference that $f_{m \rightarrow se}^i$ is not transformed into f_{re}^i , but serves as the context for MPU, for full utilization of multimodal features. With features $\{f_{CoL}^i\}_{i=4}^4$ being input to SegHead, the predicted \hat{S}_{CoL} serves as the final output.

4 Experiments

4.1 Experimental Setup

Datasets. We evaluate our method on three datasets: **DELIVER** (Zhang et al. 2023b) (general scenes with RGB, Depth, LiDAR, Event), **MCubeS** (Liang et al. 2022) (material segmentation with RGB, NIR, DoLP, AoLP), and **MUSES** (Brödermann et al. 2024) (driving scenarios with RGB, Event, LiDAR).

Baseline Methods. We compare our method with four advanced methods, *i.e.*, CMNeXt for MSS, and Any2Seg, MAGIC, AnySeg for MaSS. For equality, the backbones of all methods are set to MiT-B0 and MiT-B2 of Segformer (Xie et al. 2021). We also conduct experiments with PVTv2 (Wang et al. 2022) and Swin Transformer (Liu et al. 2021) in the *supplementary materials*. Note that results for AnySeg and Any2Seg are taken from their reports since there are no released codes or models.

Metrics. We evaluate performance using mean Intersection over Union (mIoU). *Average*, *Top-1*, and *Last-1* denote the average, best, and worst mIoU across all-modal combinations, which assess overall performance, optimal complementary effects, and degree of fragile-modal potential activation, respectively. Detailed mIoU results for all combinations are provided in the *supplementary materials*.

4.2 Qualitative Comparison

Fig. 5(a)-(c) shows the qualitative comparisons of our method with the baseline methods on the **DELIVER** dataset across different modality configurations. Results on other datasets are provided in *supplementary materials*.

- (a) **Individual Modalities:** Our method demonstrates consistent performance across all individual modalities by effectively exploiting the inherent potential of each input. It not only achieve better performance on robust modalities of RGB and Depth than the baselines, but also generate good results on fragile modalities of Event and LiDAR, on which the baselines completely fail to handle.
- (b) **Dual Modalities:** Our method exhibits superior cross-modal complementarity across various modality combinations. It achieves consistently high performance in robust+robust (R-D) settings. In robust+fragile (R-E) combinations, our method leverages Event information to compensate for RGB limitations, especially in dense tree foliage. Most notably, under the fragile+fragile setting (E-L), our method shows significant improvement in the tree region by leveraging complementary cues between Event and LiDAR.

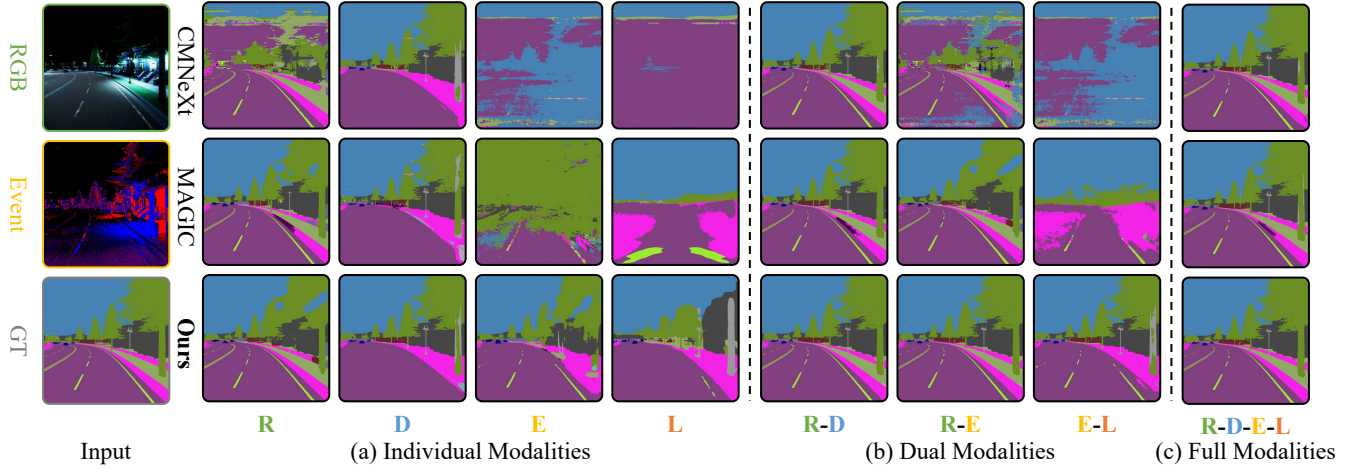


Figure 5: Visual quality comparisons of CMNeXt, MAGIC, and CHARM (Ours) on **DELIVER** dataset of different situations and arbitrary-modal combinations.

Table 1: Objective quality comparison of methods trained with datasets: **DELIVER** (four modalities), **MCubeS** (four modalities), **MUSES** (three modalities). **Bold** and underlined letter the first and second best results. “-” denotes the absence of results due to the unavailability of Any2Seg and AnySeg. All the numbers in the table are the mIoU values (%).

Backbones	Methods	DELIVER			MCubeS			MUSES		
		Average↑	Top-1↑	Last-1↑	Average↑	Top-1↑	Last-1↑	Average↑	Top-1↑	Last-1↑
Mit-B0	CMNeXt	22.05	59.18	0.37	14.35	40.94	0.46	10.80	46.66	2.64
	MAGIC	40.49	<u>63.40</u>	0.26	<u>34.56</u>	<u>47.85</u>	<u>0.55</u>	33.34	49.05	2.68
	Any2Seg	-	-	-	-	-	-	33.86	50.00	3.17
	AnySeg	47.51	59.72	<u>21.74</u>	-	-	-	<u>40.23</u>	<u>51.25</u>	<u>19.57</u>
	CHARM (Ours)	50.97	64.03	26.47	39.05	48.24	28.37	42.19	52.31	22.31
	<i>w.r.t. SOTA</i>	<i>+3.45</i>	<i>+0.63</i>	<i>+4.73</i>	<i>+4.49</i>	<i>+0.39</i>	<i>+27.82</i>	<i>+1.96</i>	<i>+1.06</i>	<i>+2.74</i>
Mit-B2	CMNeXt	25.15	66.43	<u>0.72</u>	25.17	51.54	<u>1.54</u>	33.14	<u>58.28</u>	1.23
	MAGIC	44.66	67.66	0.27	<u>38.00</u>	<u>53.01</u>	0.32	<u>36.19</u>	55.36	<u>3.34</u>
	Any2Seg	45.04	68.25	0.31	-	-	-	-	-	-
	CHARM (Ours)	54.96	68.43	28.76	46.58	54.33	38.50	46.18	59.36	25.28
	<i>w.r.t. SOTA</i>	<i>+9.92</i>	<i>+0.18</i>	<i>+28.04</i>	<i>+8.57</i>	<i>+1.32</i>	<i>+36.96</i>	<i>+9.98</i>	<i>+1.08</i>	<i>+21.93</i>

(c) **Full Modalities**: When integrating all modalities (R-D-E-L), our method also achieves superior results. While baselines misclassify part of the tree trunk as utility poles, our method correctly identifies it as vegetation, demonstrating the significant complementary effects of our mutual perception mechanism.

4.3 Quantitative Comparison

We conduct quantitative comparisons on all datasets to evaluate the effectiveness of our method across arbitrary modality combinations, as show in Tab. 1. It demonstrates that it achieves consistent improvements in *Average*, *Top-1*, and *Last-1* mIoU over all baselines, validating its robustness in handling varying modality configurations. Specifically, on **DELIVER** with Mit-B2, our method achieves 9.92% gain in *Average* mIoU over Any2Seg. Notably, it also delivers notable improvements in handling fragile modalities, with *Last-1* mIoU increasing by over 28.04% across different backbones. These consistent improvements validate the effectiveness of our complementary learning approach in collaborative harmonization across modalities.

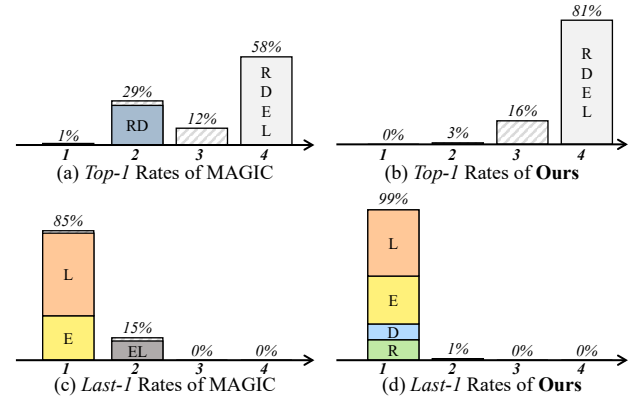


Figure 6: *Top-1* (best performance) and *Last-1* (worst performance) rates across modal combination sizes in **DELIVER**.

Fig. 6 further illustrate insights into modal combination performance by comparing our method with MAGIC. Firstly, the best results as shown in the *Top-1* rates of all modality combinations are predominantly concentrated in combination of all four modalities, while the worst results

Table 2: Ablation study on progressive component integration. The table demonstrates the cumulative benefits of each proposed module: (a) direct addition fusion baseline, (b) addition fusion with CoL, (c) addition fusion with CoL and InE, and (d) complete framework with all components. **Bold** and underlined letter the first and second best results.

Variants	Components			DELIVER			MCubeS			MUSES		
	MPU	CoL	InE	Average \uparrow	Top-1 \uparrow	Last-1 \uparrow	Average \uparrow	Top-1 \uparrow	Last-1 \uparrow	Average \uparrow	Top-1 \uparrow	Last-1 \uparrow
(a)	\times	\times	\times	33.95	63.17	2.30	25.59	45.38	3.39	30.86	51.65	2.26
(b)	\times	\checkmark	\times	41.53	62.50	3.28	33.38	46.83	14.21	31.38	51.39	0.81
(c)	\checkmark	\checkmark	\times	45.23	<u>63.97</u>	15.89	35.22	<u>47.31</u>	20.15	35.88	<u>51.96</u>	15.20
(d)	\times	\checkmark	\checkmark	48.76	62.78	24.40	36.70	46.92	26.38	38.67	51.77	19.97
(e)	\checkmark	\checkmark	\checkmark	50.97	64.03	26.47	39.05	48.24	28.37	42.19	52.31	22.31

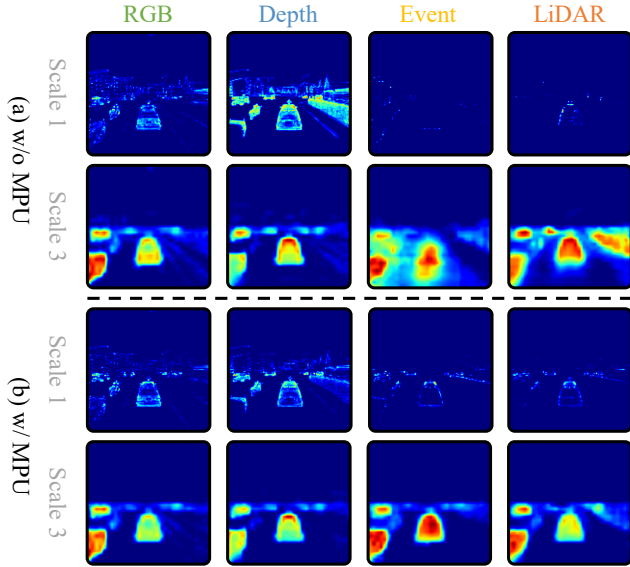


Figure 7: Feature visualization in **Variant (d)** without MPU and **Variant (e)** with MPU.

shown by the *Last-1* rates are more concentrate in the single modality in our method. This validates the effectiveness of the proposed CoL strategy in harnessing and integrating the complementary strengths of each modality, namely extra modality input can ensure better result.

Furthermore, the worst results was most in the fragile modalities of Event and Lidar from MAGIC. In our method, the worst results distribute more evenly in all modalities, owing to the reason that the InE strategy in our method has significantly boost the performance of fragile modalities by stimulating their own advantage and enhancing them through learning from other modalities.

4.4 Ablation Studies

Progressive Component Analysis. The progressive integration of components reveals their distinct functional roles and indicates the superiority of MPU-based methods over simple additive strategies. **Variant (a)** serves as the baseline with direct additive fusion, suffering from severe modality imbalance as evidenced by poor *Last-1* mIoU across all datasets. **Variant (b)** introduces CoL without MPU, showing modest improvements in average performance but still struggling with fragile-modal combinations. Comparing **Variant (c)** with **Variant (b)**, MPU-equipped methods achieve significant gains in *Average* and *Top-1* mIoU, demonstrat-

ing MPU’s effectiveness in handling fragile-modal scenarios. This superiority stems from MPU’s mutual perception mechanism that iteratively inherits complementary content from all modalities, preventing information-rich robust modalities from being diluted by information-sparse fragile modalities as occurs in additive fusion. **Variant (d)** incorporates InE alongside CoL, providing protective mechanism that further alleviate performance suppression of fragile modalities, validated by the improvements in *Last-1* mIoU. **Variant (e)** achieves optimal performance by integrating all components, where MPU harmonizes cross-modal interactions while CoL enables robust complementary fusion and InE ensures individual modal enhancement.

To further validate MPU’s capability in collaborative harmonization, we visualize the features by Grad-CAM (Selvaraju et al. 2017) in **Variant (d)** without MPU and **Variant (e)** with MPU in Fig. 7. It shows that at Scale 1, robust modalities (RGB, Depth) show significantly improved on target vehicles with enhanced textural cues extraction, while fragile modalities (Event, LiDAR) show reduced noise and more concentrated responses. At Scale 3, all modalities exhibit substantially refined attention patterns, with Event and LiDAR showing markedly reduced diffusion in irrelevant regions while maintaining their unique semantic contributions. This cross-modal mutual perception mechanism enables each modality to leverage contextual information from others, leading to enhanced discriminative power for robust modalities and focused representational domains for fragile modalities. This validates that MPU enables maximum texture extraction in shallow layers and facilitates semantic exchange without mutual suppression in deeper layers, successfully achieving harmonization rather than homogenization while preserving modality-specific strengths.

Comparison between MPU with Explicit Alignment. To demonstrate the effectiveness of MPU in promoting implicit alignment, we replace the MPU by a explicit alignment that applies KL divergence loss at each scale to force multimodal features toward their average representation. The visualization in Fig. 8 reveals clear differences in activation patterns: explicit alignment unit forces all modalities toward centralized representations causing universal degradation. In contrast, MPU maintains distinctive yet complementary activation patterns across modalities. The red boxes illustrate ineffective learning in fragile modalities under explicit constraints, where the model captures features beyond its inherent capacity at Scale 1. The green boxes show degraded activations in robust modalities at Scale 3, with scattered and weakened responses due to forced alignment. In contrast,

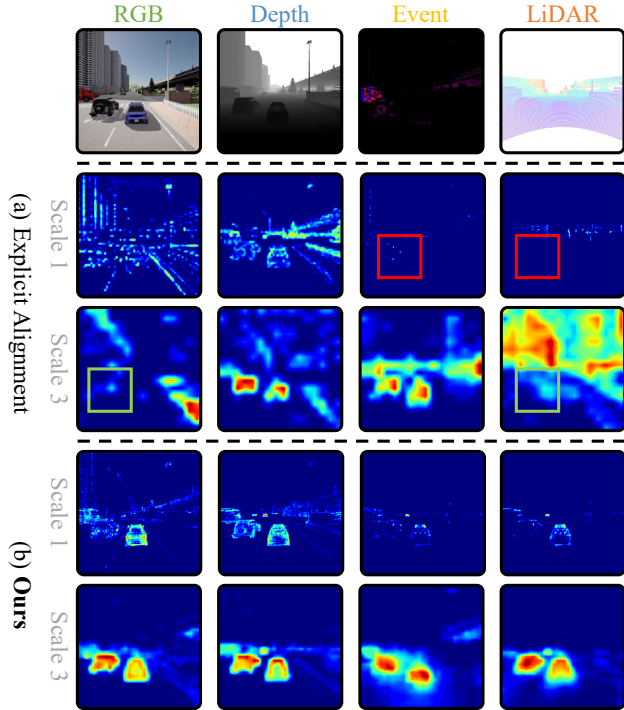


Figure 8: Feature visualization across different strategies. Colored boxes highlight different failure modes.

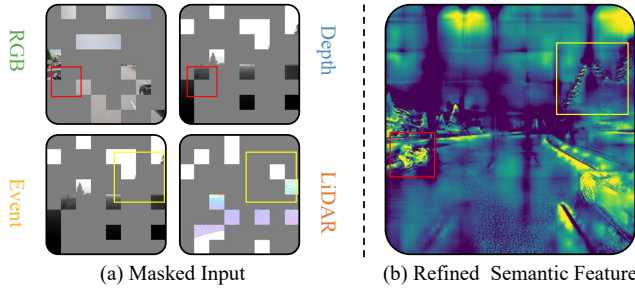


Figure 9: Visualization for multimodal complementarity. (a) Random masking inputs four modalities. (b) Feature visualization at Scale 3.

MPU preserves the representational integrity of each modality across both shallow and deep layers, enabling effective cross-modal cooperation without suppressing modality-specific strengths.

Abilities in Complementary Fusion. Our method enables complementary fusion by selectively integrating distinctive information from different modalities based on their inherent strengths. Fig. 9(a) shows how our method effectively extracts and fuses key information using a masking strategy that retains only complementary information blocks from each modality. Fig. 9(b) further illustrates the complementary fusion process: features of the motorcycle (red box) are primarily derived from RGB and Depth, leveraging their strong object recognition and spatial understanding capabilities, while features of the tree (yellow box) are captured from Event and LiDAR, which capture their temporal dynamics and precise geometry. This validates that our

method enables maximum texture extraction in shallow layers and facilitates semantic exchange in deeper layers without suppressing modality-specific representations, achieving harmonization rather than homogenization.

5 Conclusion

This paper identifies that current MaSS methods pursue multimodal homogenization, leading to diluted representations and suppressed complementary characteristics. To address it, we propose CHARM, a cooperative framework that achieves harmonization through two key innovations. The first is the fundamental MPU that enables discovering modality-interactive correspondences without explicit alignment constraints. Secondly, CoL and InE strategies provide systematic balance between collaborative learning and individual modal enhancement, ensuring optimal utilization of each modality’s unique potential through robustness-guided cooperation. The consistent gains across different datasets and backbones confirm that our cooperative paradigm successfully preserves modal distinctiveness, and ensures the robust Mass performance by improving the effectiveness of each modality and various modality combinations in the modality-agnostic settings.

References

- Alonso, I.; and Murillo, A. C. 2019. EV-SegNet: Semantic Segmentation for Event-Based Cameras. In *2019 IEEE/CVF Conference on Computer Vision and Pattern Recognition Workshops (CVPRW)*, 1624–1633.
- Brödermann, T.; Bruggemann, D.; Sakaridis, C.; Ta, K.; Liagouris, O.; Corkill, J.; and Van Gool, L. 2024. MUSES: The Multi-sensor Semantic Perception Dataset for Driving Under Uncertainty. In *2024 European Conference on Computer Vision (ECCV)*, 21–38.
- Brödermann, T.; Sakaridis, C.; Dai, D.; and Van Gool, L. 2023. HRFuser: A Multi-Resolution Sensor Fusion Architecture for 2D Object Detection. In *2023 IEEE 26th International Conference on Intelligent Transportation Systems (ITSC)*, 4159–4166.
- Chen, Y.; Zhao, M.; and Bruzzone, L. 2024. A Novel Approach to Incomplete Multimodal Learning for Remote Sensing Data Fusion. *IEEE Transactions on Geoscience and Remote Sensing*, 62: 1–14.
- Dong, S.; Zhou, W.; Xu, C.; and Yan, W. 2024. EGFNet: Edge-aware Guidance Fusion Network for RGB–Thermal Urban Scene Parsing. *IEEE Transactions on Intelligent Transportation Systems*, 25(1): 657–669.
- Feng, Z.; Xiong, H.; Min, W.; Hou, S.; Duan, H.; Liu, Z.; and Jiang, S. 2024. Ingredient-Guided RGB-d Fusion Network for Nutritional Assessment. *IEEE Transactions on AgriFood Electronics*, 1–11.
- Gao, S.; Yang, X.; Jiang, L.; Fu, Z.; and Du, J. 2024. Global Feature-Based Multimodal Semantic Segmentation. *Pattern Recognition*, 151: 110340.
- Li, B.; Zhang, D.; Zhao, Z.; Gao, J.; and Li, X. 2024. Stitch-Fusion: Weaving Any Visual Modalities to Enhance Multimodal Semantic Segmentation. arXiv:2408.01343.

- Liang, Y.; Wakaki, R.; Nobuhara, S.; and Nishino, K. 2022. Multimodal Material Segmentation. In *2022 IEEE/CVF Conference on Computer Vision and Pattern Recognition (CVPR)*, 19768–19776.
- Liu, R.; Zhang, J.; Peng, K.; Chen, Y.; Cao, K.; Zheng, J.; Sarfraz, M. S.; Yang, K.; and Stiefelhofen, R. 2024. Fourier Prompt Tuning for Modality-Incomplete Scene Segmentation. In *2024 IEEE Intelligent Vehicles Symposium (IV)*, 961–968.
- Liu, Z.; Lin, Y.; Cao, Y.; Hu, H.; Wei, Y.; Zhang, Z.; Lin, S.; and Guo, B. 2021. Swin Transformer: Hierarchical Vision Transformer Using Shifted Windows. In *2021 IEEE/CVF International Conference on Computer Vision (ICCV)*, 9992–10002.
- Maheshwari, H.; Liu, Y.-C.; and Kira, Z. 2024. Missing Modality Robustness in Semi-Supervised Multi-Modal Semantic Segmentation. In *2024 IEEE/CVF Winter Conference on Applications of Computer Vision (WACV)*, 1009–1019.
- Mei, H.; Dong, B.; Dong, W.; Yang, J.; Baek, S.-H.; Heide, F.; Peers, P.; Wei, X.; and Yang, X. 2022. Glass Segmentation Using Intensity and Spectral Polarization Cues. In *2022 IEEE/CVF Conference on Computer Vision and Pattern Recognition (CVPR)*, 12612–12621.
- Reza, M. K.; Prater-Bennette, A.; and Asif, M. S. 2024. MMSFormer: Multimodal Transformer for Material and Semantic Segmentation. *IEEE Open Journal of Signal Processing*, 5: 599–610.
- Selvaraju, R. R.; Cogswell, M.; Das, A.; Vedantam, R.; Parikh, D.; and Batra, D. 2017. Grad-CAM: Visual Explanations from Deep Networks via Gradient-Based Localization. In *2017 IEEE International Conference on Computer Vision (ICCV)*, 618–626.
- Sharma, A.; and Hamarneh, G. 2020. Missing MRI Pulse Sequence Synthesis Using Multi-Modal Generative Adversarial Network. *IEEE Transactions on Medical Imaging*, 39(4): 1170–1183.
- Shi, J.; Shang, C.; Sun, Z.; Yu, L.; Yang, X.; and Yan, Z. 2024. PASSION: Towards Effective Incomplete Multi-Modal Medical Image Segmentation with Imbalanced Missing Rates. In *Proceedings of the 32nd ACM International Conference on Multimedia*, 456–465.
- Tan, M.; Zhuang, Z.; Chen, S.; Li, R.; Jia, K.; Wang, Q.; and Li, Y. 2024. EPMF: Efficient Perception-Aware Multi-Sensor Fusion for 3D Semantic Segmentation. *IEEE Transactions on Pattern Analysis and Machine Intelligence*, 46(12): 8258–8273.
- Wan, Z.; Zhang, P.; Wang, Y.; Yong, S.; Stepputtis, S.; Sycara, K.; and Xie, Y. 2024. Sigma: Siamese Mamba Network for Multi-Modal Semantic Segmentation.
- Wang, H.; Ma, C.; Zhang, J.; Zhang, Y.; Avery, J.; Hull, L.; and Carneiro, G. 2023. Learnable Cross-modal Knowledge Distillation for Multi-modal Learning with Missing Modality. In *Medical Image Computing and Computer Assisted Intervention – MICCAI 2023: 26th International Conference, Vancouver, BC, Canada, October 8–12, 2023, Proceedings, Part IV*, 216–226. Berlin, Heidelberg: Springer-Verlag. ISBN 978-3-031-43900-1.
- Wang, W.; Xie, E.; Li, X.; Fan, D.-P.; Song, K.; Liang, D.; Lu, T.; Luo, P.; and Shao, L. 2022. PVT v2: Improved Baselines with Pyramid Vision Transformer. *Computational Visual Media*, 8(3): 415–424.
- Wei, S.; Zhou, Z.; Lu, Z.; Yuan, Z.; and Su, B. 2025. HDBFormer: Efficient RGB-d Semantic Segmentation with a Heterogeneous Dual-Branch Framework. *IEEE Signal Processing Letters*, 32: 91–95.
- Xia, R.; Zhao, C.; Zheng, M.; Wu, Z.; Sun, Q.; and Tang, Y. 2023. CMDA: Cross-modality Domain Adaptation for Nighttime Semantic Segmentation. In *2023 IEEE/CVF International Conference on Computer Vision (ICCV)*, 21515–21524.
- Xie, E.; Wang, W.; Yu, Z.; Anandkumar, A.; Alvarez, J. M.; and Luo, P. 2021. SegFormer: Simple and Efficient Design for Semantic Segmentation with Transformers. In *Proceedings of the 35th International Conference on Neural Information Processing Systems (NeurIPS)*, 12077–12090.
- Yang, B.; Guo, Y.; Ni, R.; Liu, Y.; Li, G.; and Hu, C. 2025. Asymmetric Multimodal Guidance Fusion Network for Realtime Visible and Thermal Semantic Segmentation. *Engineering Applications of Artificial Intelligence*, 142: 109881.
- Zhang, J.; Liu, H.; Yang, K.; Hu, X.; Liu, R.; and Stiefelhofen, R. 2023a. CMX: Cross-Modal Fusion for RGB-X Semantic Segmentation With Transformers. *IEEE Transactions on Intelligent Transportation Systems*, 24(12): 14679–14694.
- Zhang, J.; Liu, R.; Shi, H.; Yang, K.; Reiß, S.; Peng, K.; Fu, H.; Wang, K.; and Stiefelhofen, R. 2023b. Delivering Arbitrary-Modal Semantic Segmentation. In *2023 IEEE/CVF Conference on Computer Vision and Pattern Recognition (CVPR)*, 1136–1147.
- Zhang, Y.; He, N.; Yang, J.; Li, Y.; Wei, D.; Huang, Y.; Zhang, Y.; He, Z.; and Zheng, Y. 2022. mmFormer: Multimodal Medical Transformer for Incomplete Multimodal Learning of Brain Tumor Segmentation. In *2022 Medical Image Computing and Computer Assisted Intervention (MICCAI)*, 107–117.
- Zhang, Y.; Li, N.; Jiao, J.; Ai, J.; Yan, Z.; Zeng, Y.; Zhang, T.; and Li, Q. 2025a. CMFFN: An Efficient Cross-Modal Feature Fusion Network for Semantic Segmentation. *Robotics and Autonomous Systems*, 186: 104900.
- Zhang, Z.; Wang, W.; Zhu, L.; and Tang, Z. 2025b. TAG-fusion: Two-stage Attention Guided Multi-Modal Fusion Network for Semantic Segmentation. *Digital Signal Processing*, 156(PA).
- Zheng, X.; Lyu, Y.; Jiang, L.; Zhou, J.; Wang, L.; and Hu, X. 2024a. MAGIC++: Efficient and Resilient Modality-Agnostic Semantic Segmentation via Hierarchical Modality Selection. arXiv:2412.16876.
- Zheng, X.; Lyu, Y.; and Wang, L. 2025. Learning Modality-Agnostic Representation for Semantic Segmentation from Any Modalities. In *2024 European Conference on Computer Vision (ECCV)*, 146–165.

Zheng, X.; Lyu, Y.; Zhou, J.; and Wang, L. 2024b. Centering the Value of Every Modality: Towards Efficient and Resilient Modality-Agnostic Semantic Segmentation. In *European Conference on Computer Vision (ECCV)*, 192–212.

Zheng, X.; Xue, H.; Chen, J.; Yan, Y.; Jiang, L.; Lyu, Y.; Yang, K.; Zhang, L.; and Hu, X. 2025. Learning Robust Anymodal Segmentor with Unimodal and Cross-modal Distillation. arXiv:2411.17141.